Electronic Supplementary Material (ESI) for Dalton Transactions.

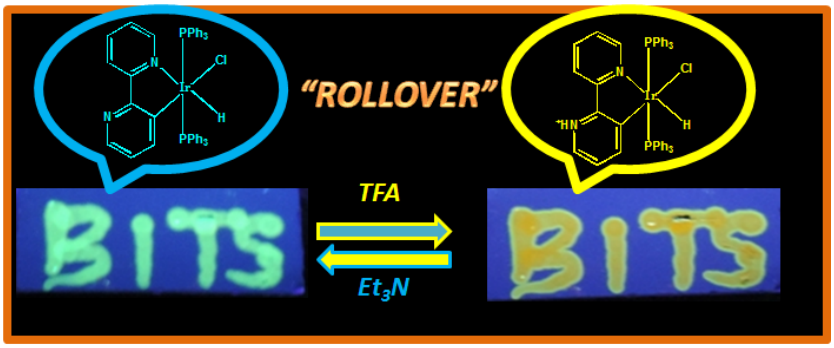

An 'aggregation induced phosphorescence (AIP)' active rollover complex was synthesized and verified its capability as Multi-Stimuli-Responsive smart luminescence material.

SUPPELEMENTARY DATA

‘Aggregation Induced Phosphorescence’ Active ‘Rollover’ Iridium(III) Complex as Multi-Stimuli-Responsive Luminescence Material

Parvej Alam[a], Gurpreet Kaur[b], Shamik chakrowarty[a],Angshuman Roy Choudhury[b]*, Inamur Rahaman Laskar[a]*

[a]Department of Chemistry, Birla Institute of Technology and Science, Pilani Campus, Pilani, Rajasthan, India, ir_laskar@bits-pilani.ac.in; [b]Department of Chemical Sciences, Indian Institute of Science Education and Research (IISER), Mohali, Sector 81, S. A. S. Nagar, Manauli PO, Mohali, Punjab, 140306, India, angshurc@iisermohali.ac.in;

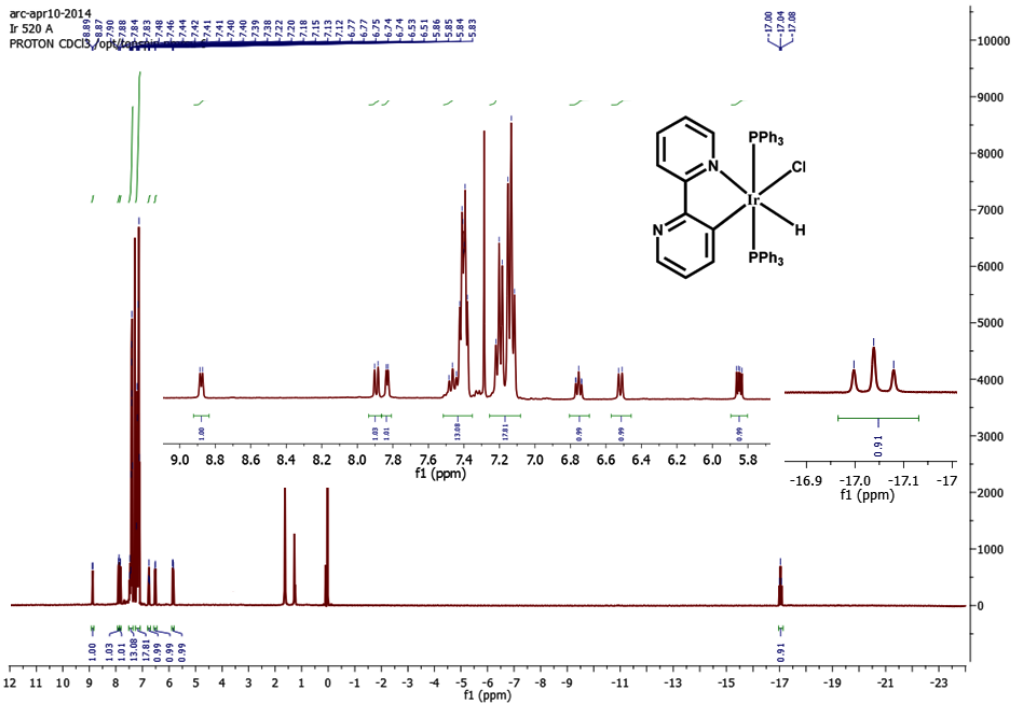

a

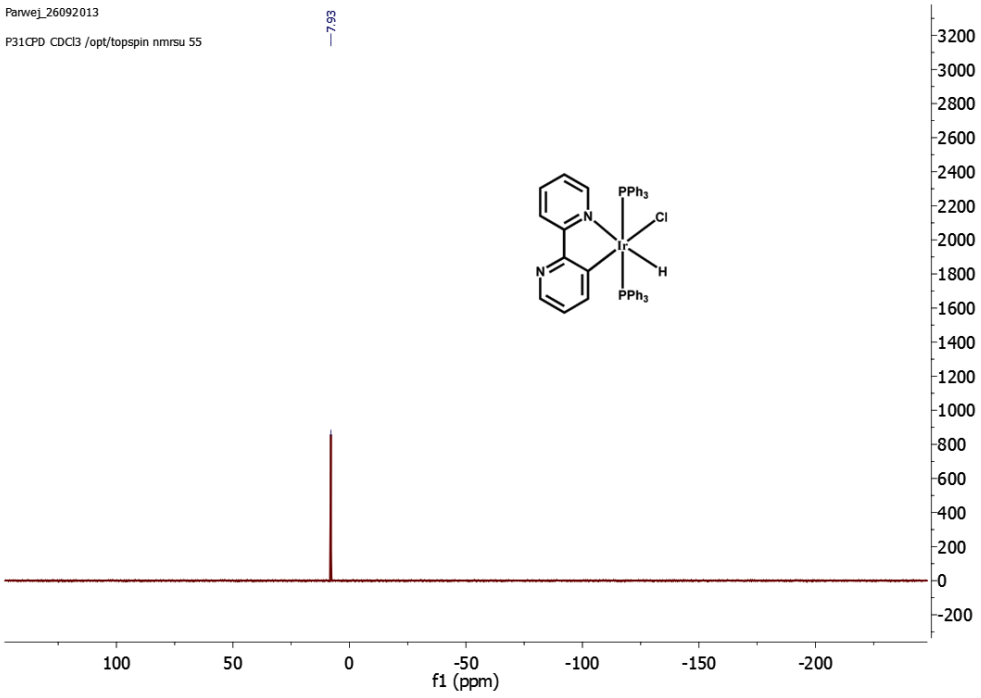
Parwej_26092013
P31CPD CDCl3 /opt/topspin nmrsu 55
7.93
PPh3
Cl
Ir
H
PPh3
N
N
3200
3000
2800
2600
2400
2200
2000
1800
1600
1400
1200
1000
800
600
400
200
0
-200
100
50
0
-50
-100
-150
-200
f1 (ppm)

b

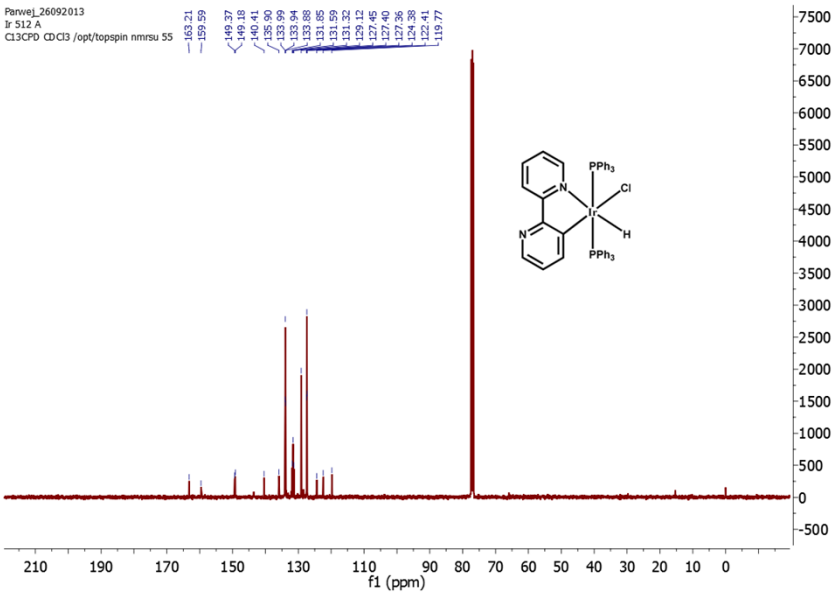
Parwej_26092013
Ir 512 A
C13CPD CDCl3 /opt/topspin nmrsu 55
163.21
159.59
149.37
149.18
140.41
135.90
133.99
133.94
133.88
131.85
131.59
131.32
129.12
127.45
127.40
127.36
124.38
122.41
119.77
PPh3
Cl
Ir
H
PPh3
N
N
7500
7000
6500
6000
5500
5000
4500
4000
3500
3000
2500
2000
1500
1000
500
0
-500
210
190
170
150
130
110
90
80
70
60
50
40
30
20
10
0
f1 (ppm)

c

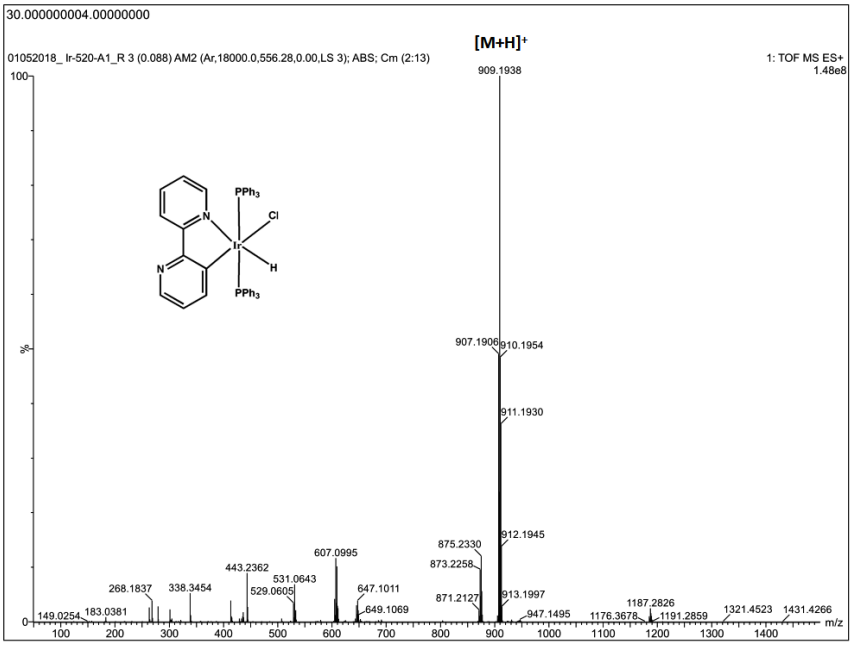

Fig. S1 (^{1}H, ^{31}P,^{13}C) NMR spectra and HRMS (a, b, c and d), respectively for [Ir(bipy-H)].

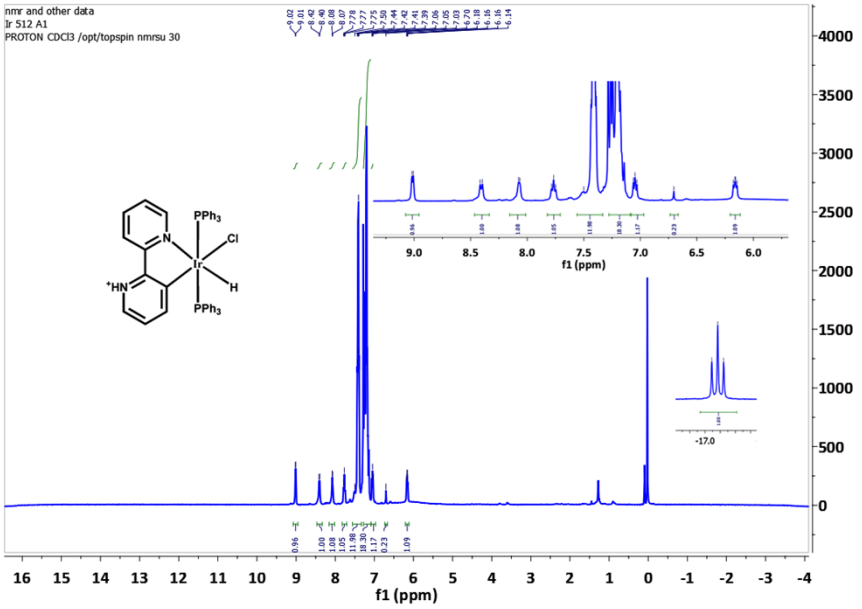
nmr and other data
Ir 512 A1
PROTON CDCl3 /opt/topspin nmrsu 30
PPh3
Cl
Ir
N
+HN
H
PPh3
f1 (ppm)

a

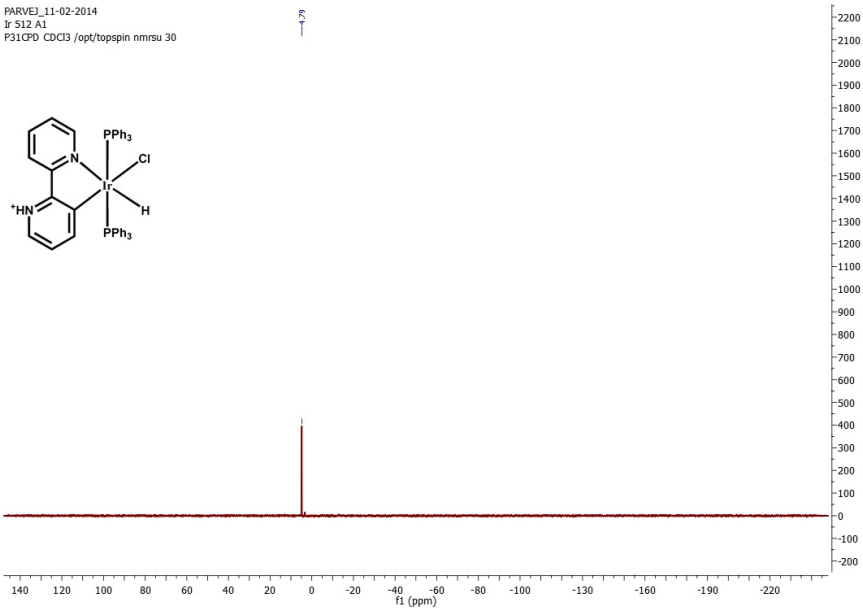
PARVEJ_11-02-2014
Ir 512 A1
P31CPD CDCl3 /opt/topspin nmrsu 30
-4.79
PPh3
Cl
Ir
N
+HN
H
PPh3
f1 (ppm)

b

Fig.S2 (^{1}H and ^{31}P,) NMR spectra (**a**, **b)**, respectively for [Ir(bipy-H)H^{+}] in $CDCl_3$.

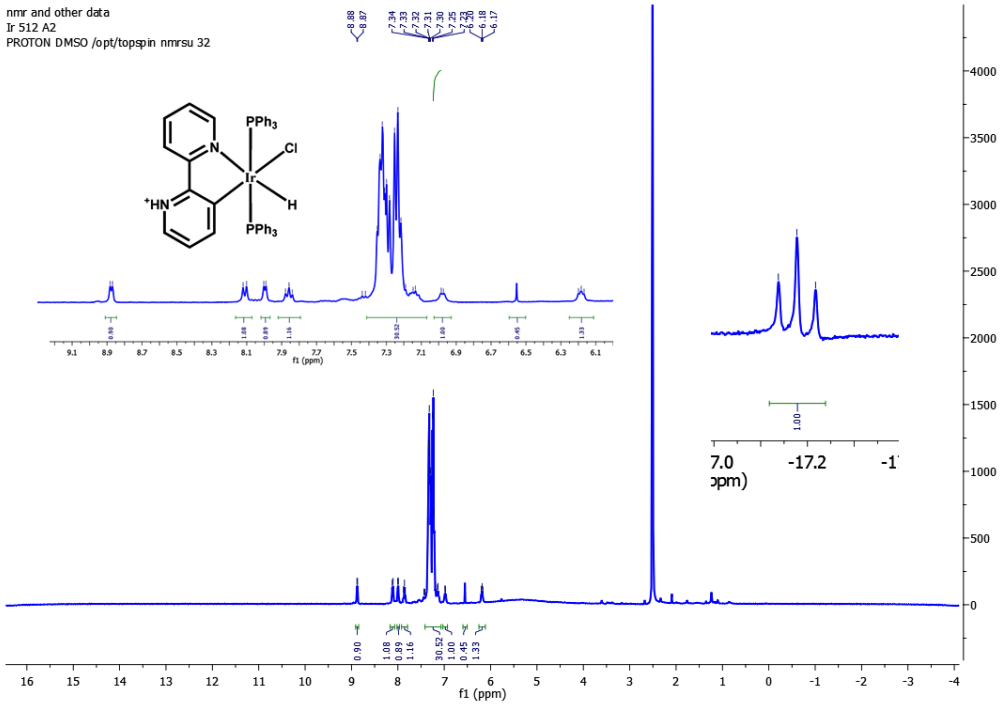

a

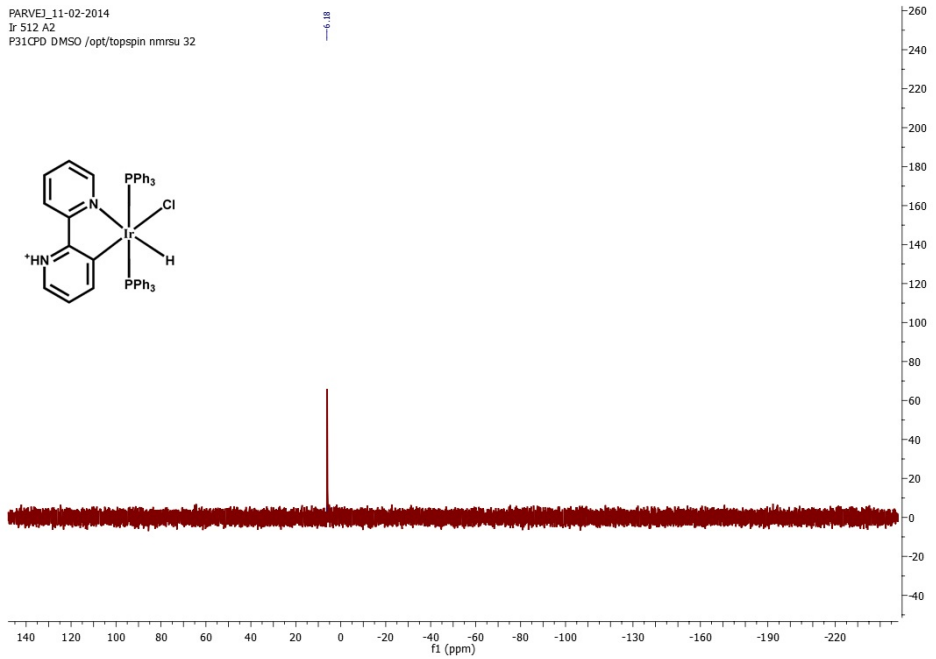

b

Fig.S3 (^{1}H and ^{31}P,) NMR spectra (**a**, **b)**, respectively for [Ir(bipy-H)H^{+}] in DMSO-d_6.

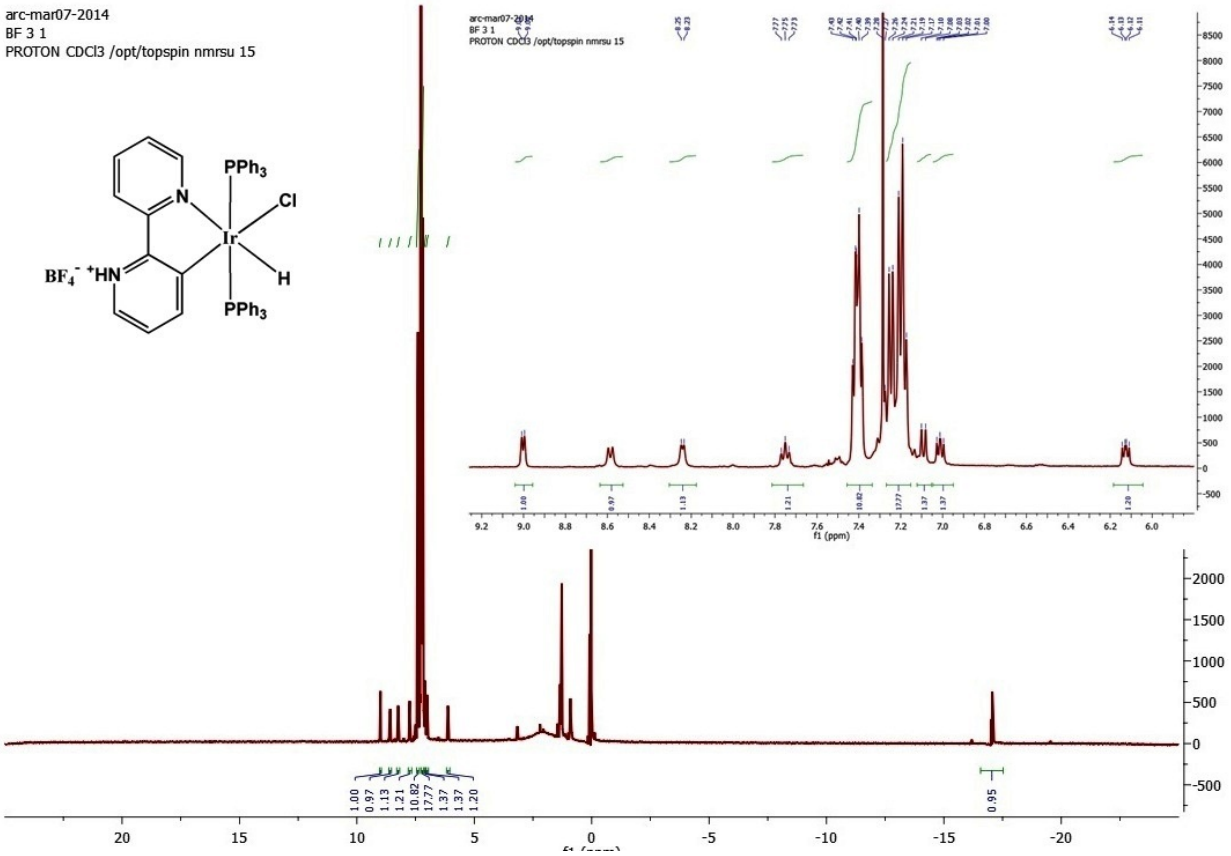
arc-mar07-2014
BF 3 1
PROTON CDCl3 /opt/topspin nmrsu 15
PPh3
Cl
N
Ir
BF4- +HN
H
PPh3
f1 (ppm)

a

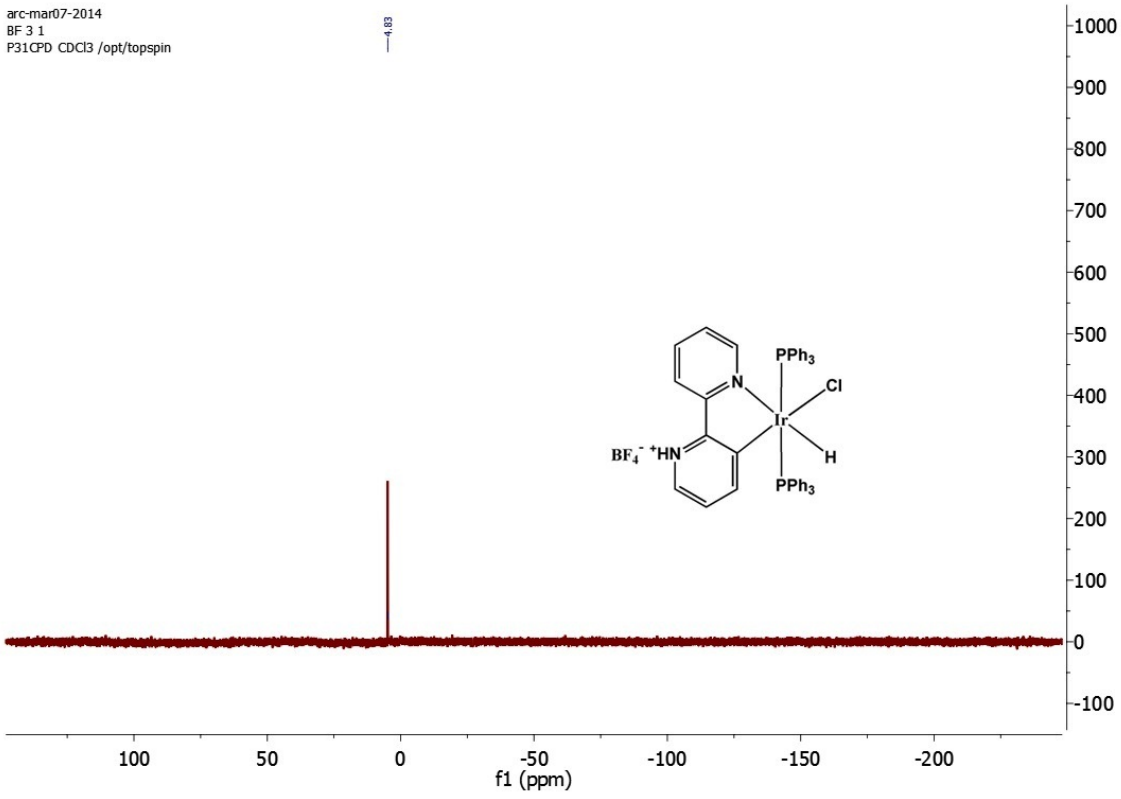

b

Fig.S4 (^{1}H, ^{31}P,) NMR spectra (**a** and **b**), respectively for [Ir(bipy-H)H^{+} BF_4^{-}] in $CDCl_3$.

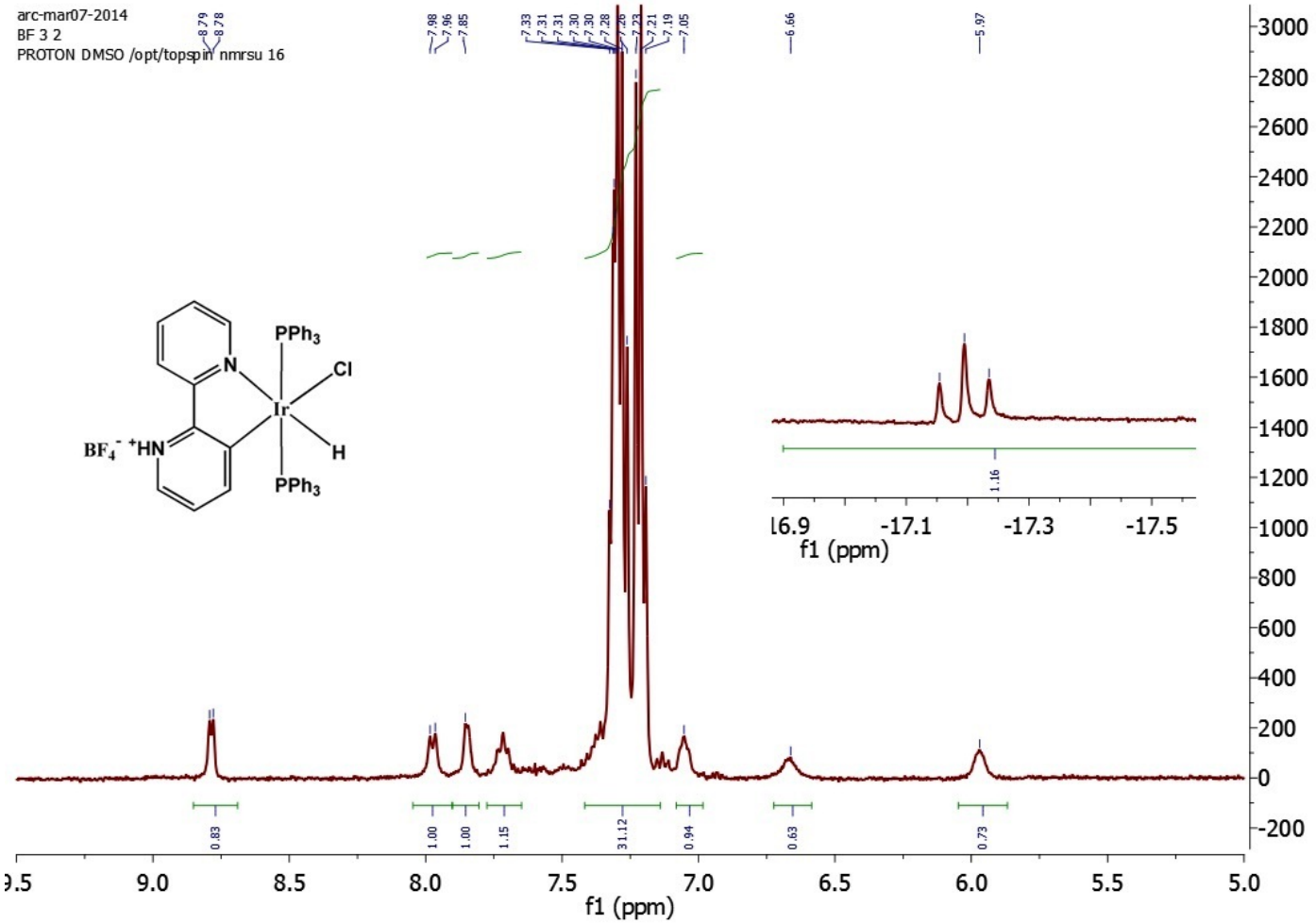
arc-mar07-2014
BF 3 2
PROTON DMSO /opt/topspin nmrsu 16
PPh3
Cl
N
Ir
BF4- +HN
H
PPh3
f1 (ppm)
f1 (ppm)

a

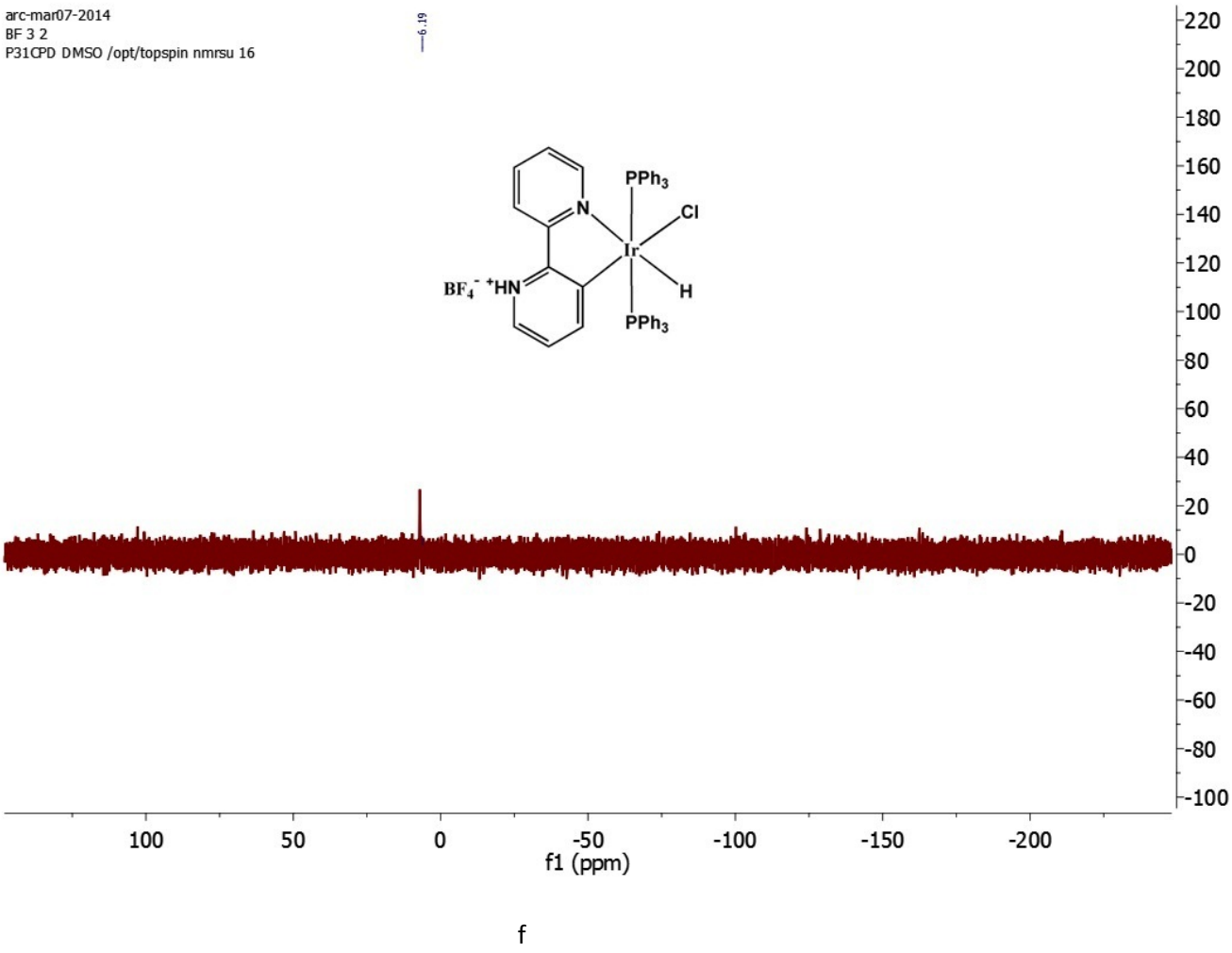

f

Fig.S5 (^{1}H, ^{31}P,) NMR spectra (**a** and **b**), respectively for [Ir(bipy-H)$H^{+}BF_4^{-}$] in DMSO-d_6 .

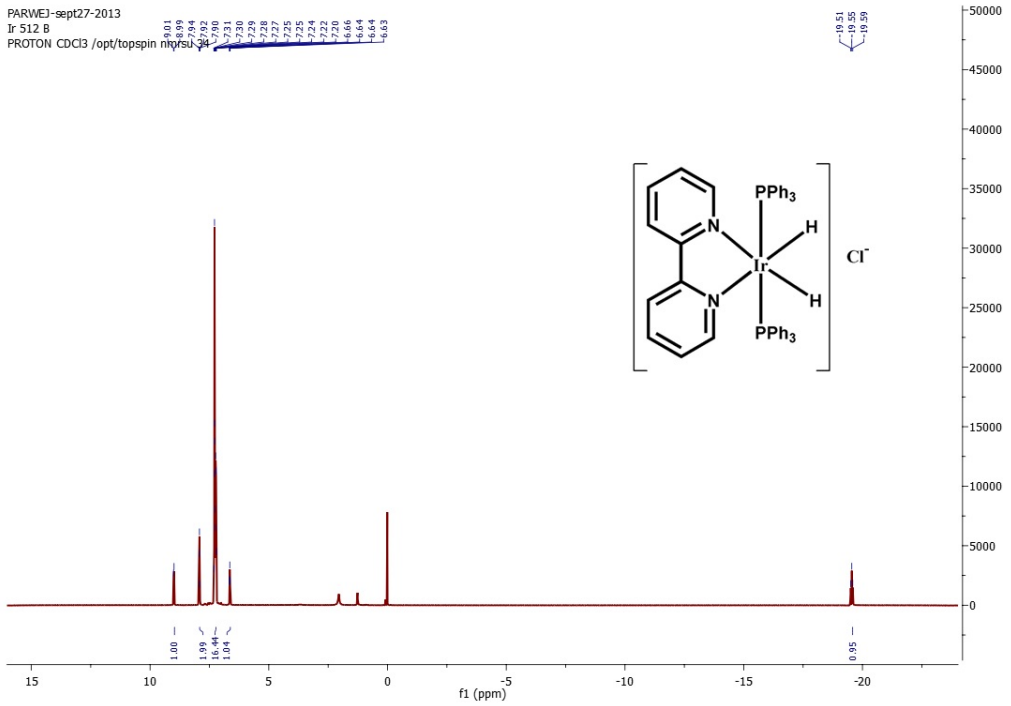

Fig.S6 ^{1}H, NMR spectra for [**Ir(bipy)(H_2)(PPh_3)$_2$]**

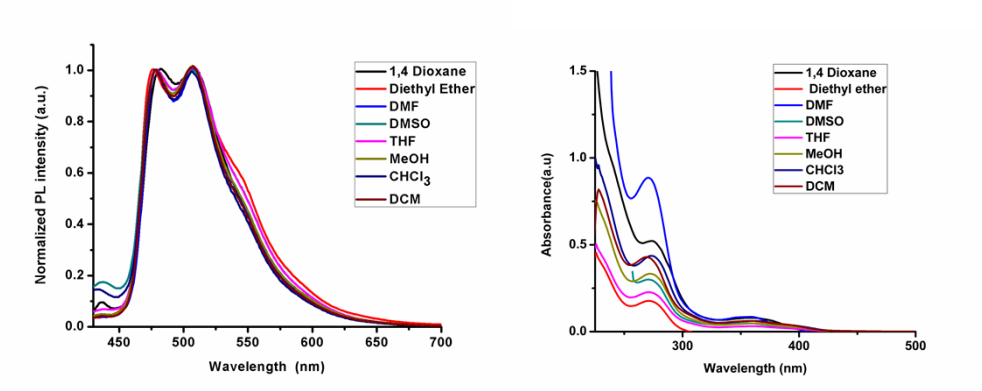

a b

Fig.S7 Emission and Absorption spectra of [Ir(bipy-H)] in different solvents.

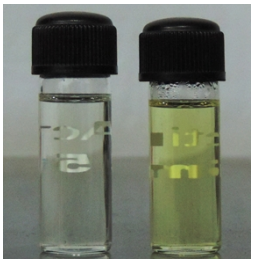

Fig.S8 photo of [Ir(bipy-H)] in DCM (left) and DCM +TFA (right) under day light.

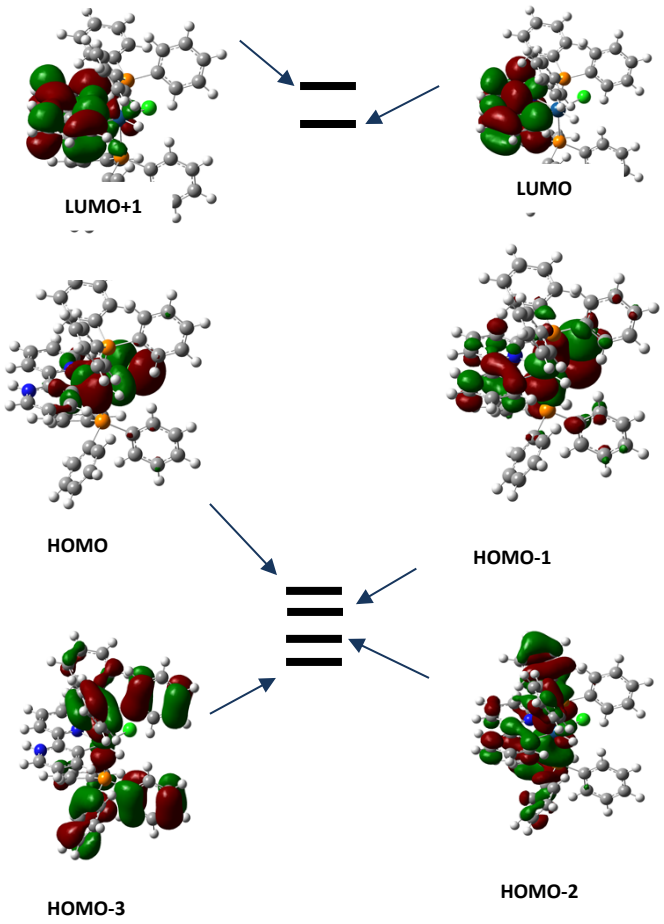

Fig.S9 Highest and lowest occupied molecular orbitals of [Ir(bipy-H)H^{+}]

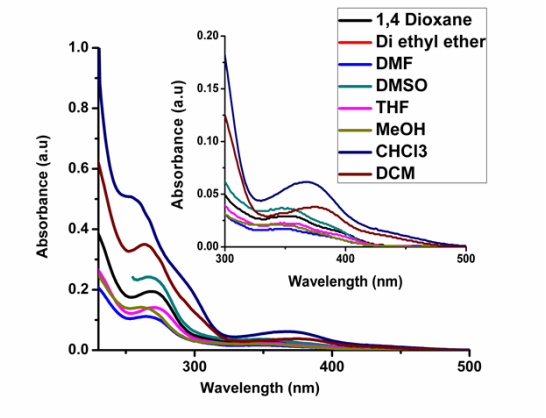

Fig.S10 Absorbance spectra of [Ir(bipy-H)H$^+$] in different solvents.

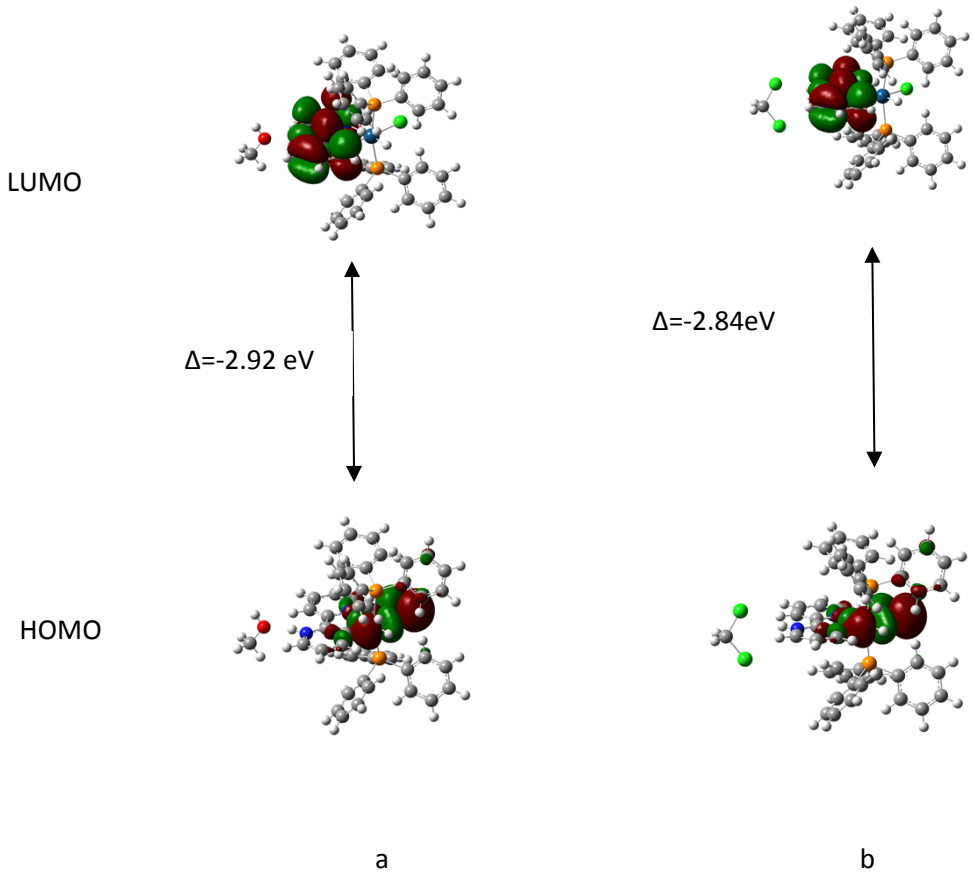

Fig.S11 Highest and lowest occupied molecular orbitals of (a) [Ir(bipy-H)H$^+$]·MeOH and (b) [Ir(bipy-H)H$^+$]·DCM

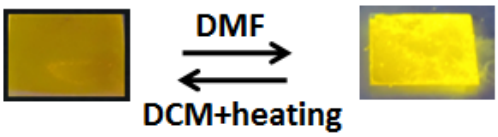

a

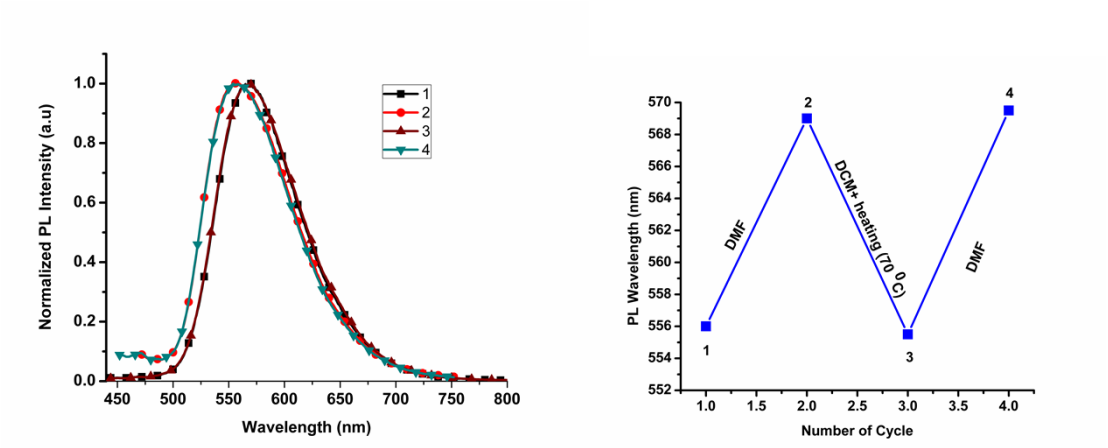

i ii

b

Fig. S12. Solid-state reversal of emission color of [Ir(bipy-H)H$^+$] from orangish yellow to yellow (on exposure to DMF) and orangish yellow to yellow (on exposure to DCM with 50 ^{0}C heating) (the photograph was taken under excitation of 364nm); **b (1).** Reversibility of solid-state emission spectrum of [Ir(bipy-H)H$^+$] with repeated VOC exposure (2, on exposure to DMF; (3, on exposure to DCM after heating the film at 70°C for 10 min and (4, on exposure to DMF); **(2)**. Switching of emission wavelength (~569 nm to ~555 nm and vice versa) on exposure to DMF and DCM repeatedly, respectively

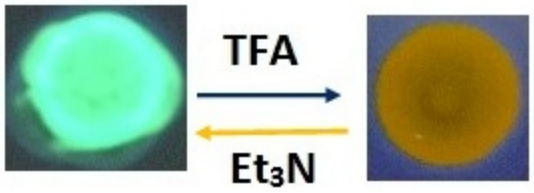

a

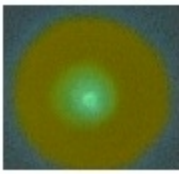

b

Fig. S13 (a) The TLC plate Image of [Ir(bipy-H)] , the greenish blue emission color of the complex is converted into yellowish orange color after the exposure of TFA and convert back to greenish blue after exposure of Et_3N(fully reversible in nature) **(b)** A small drop of Et_3N on TLC plate containing [Ir(bipy-H)H^+] showing the partial colour change.

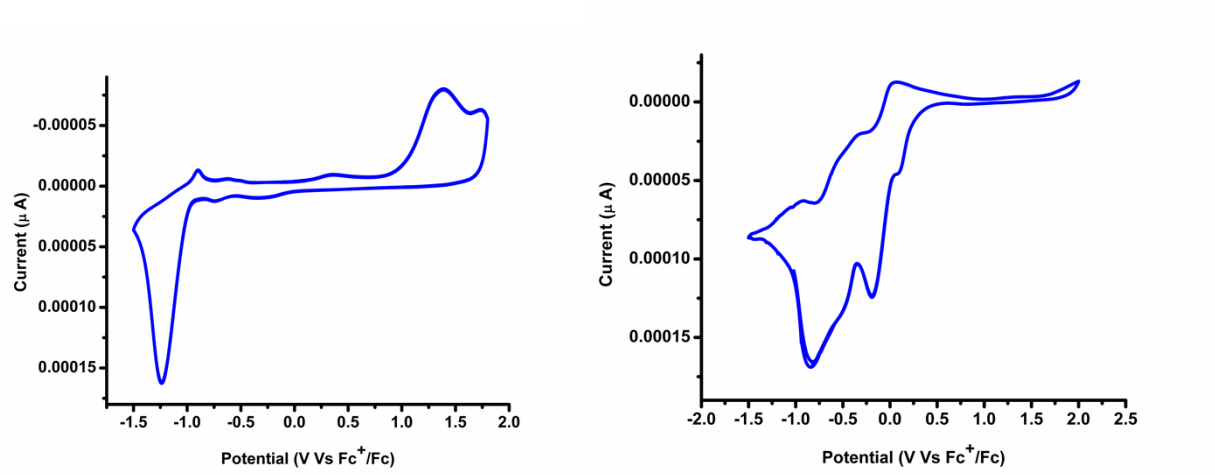

a b

Fig.S14 Cyclic voltammogram of [Ir(bipy-H)] (a) and of [Ir(bipy-H)H^{+}] (b) respectively, recorded in ACN at a scan rate of 0.05 V s^{-1}

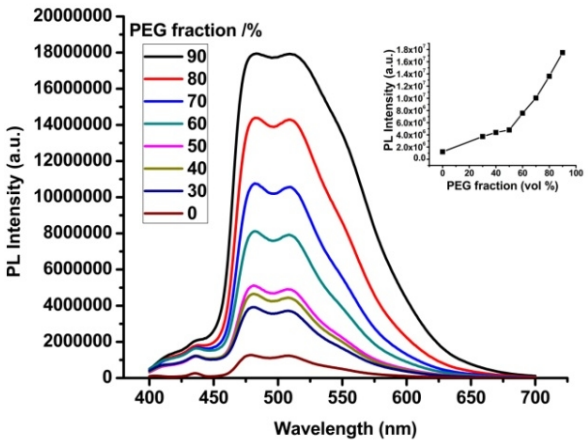

Fig.S15 PL spectra of [Ir(bipy-H)] with [M] =10^{-5} mol L^{-1} in THF–PEG mixtures , PEG fraction (f_{PEG})

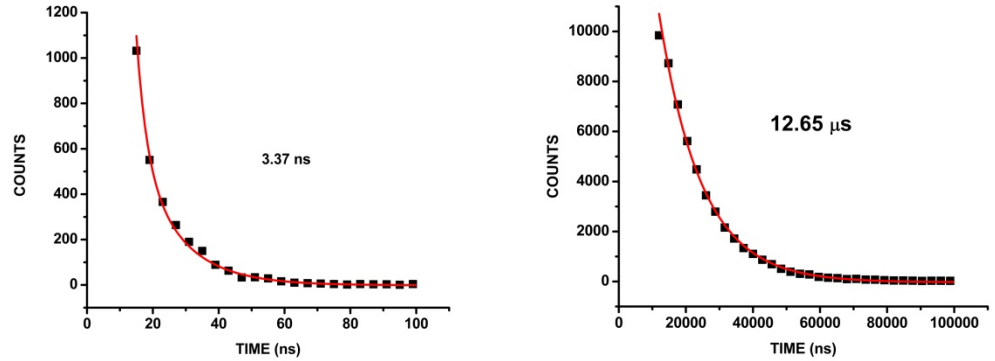

a b

Fig. S16 Photoluminescence lifetime decay curves (a) in THF and (b) in f_w=95% for [Ir(bipy-H)] (the red line is the fitting curve).

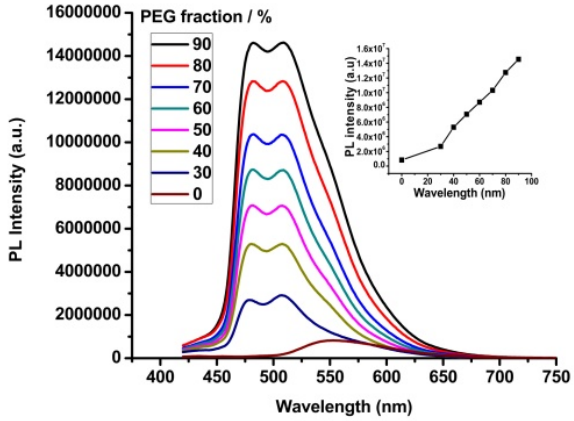

Fig. S17 PL spectra of [Ir(bipy-H)H^+] with [M] =10^{-5} mol L^{-1} in THF–PEG mixtures , PEG fraction (f_{PEG})

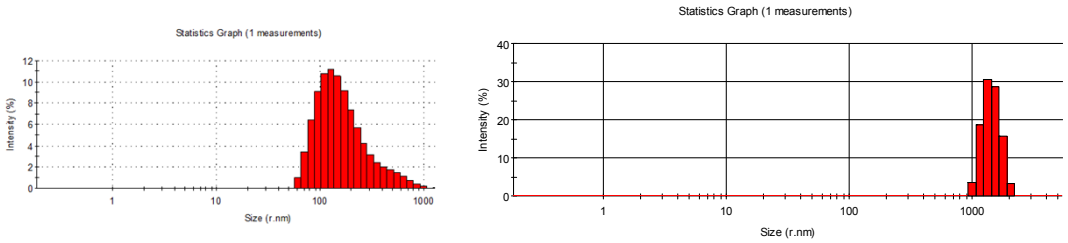

a b

Fig. S18 (a) Particle size distribution of nano-aggregates of complexes)] in a THF/ water mixture with a 90% water fraction (a) [Ir(bipy-H)] (b) [Ir(bipy-H)H^+]

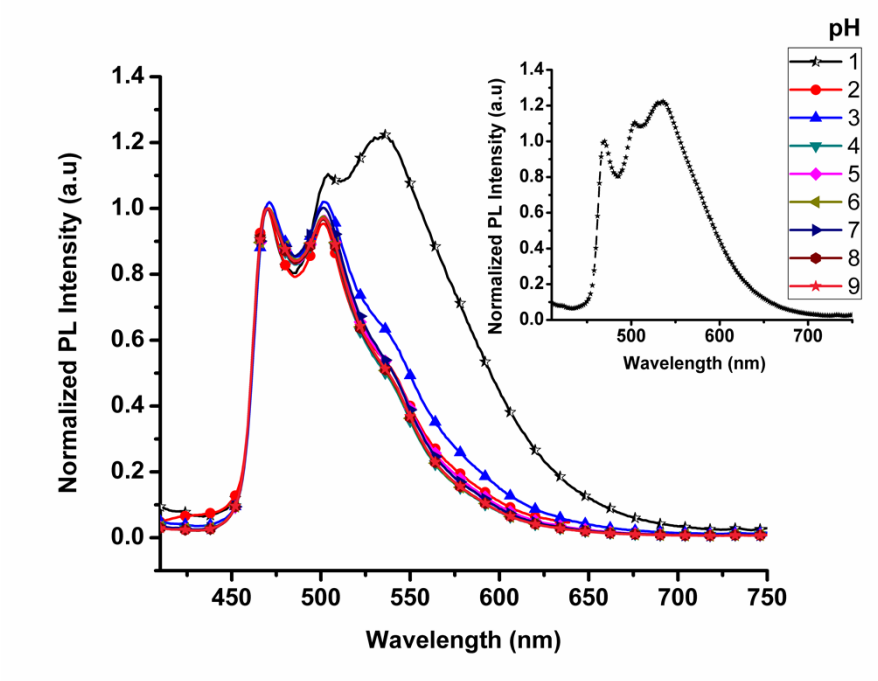

a

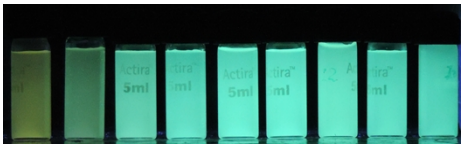

B

Fig. S19 (a). Emission spectra of [Ir(bipy-H)] in THF buffer mixture with different pH (1-9) (b) photo of the buffer solutions with THF, f_w =90% (pH= 1-9) under 365 nm UV lamp.

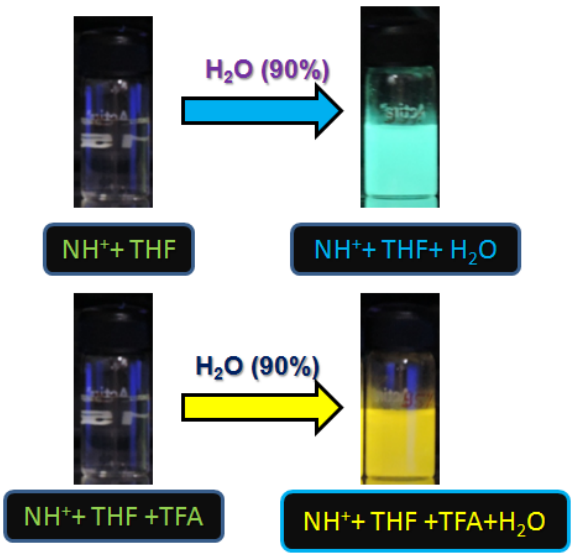

Fig. S20 (a) Emission spectra of [Ir(bipy-H)] in THF buffer mixture with different pH (1-9) (b) photo of the buffer solutions with THF, f_w =90% (pH= 1-9) under 365 nm UV lamp.

Table 1. Geometrical parameters for the coordination environment of Iridium in the optimized ground state structures of compounds [Ir(bipy-H)] and [Ir(bipy-H)H^+] in dichloromethane solution.

Bond length	**(Exp.)**	**(Theoretical)**	**Bond angle**	**(Exp.)**	**(Theoretical)**
	[Ir(bipy-H)H^+]	[Ir(bipy-H)H^+]		[Ir(bipy-H)H^+]	[Ir(bipy-H)H^+]
Ir-P1	2.339	2.405	P1IrP2	174.21	168.02
Ir-P2	2.330	2.403	P1IrC	89.20	93.95
Ir-N	2.167	2.232	P1IrCl	89.49	86.92
Ir-C	1.994	2.022	P1IrN	95.15	94.92
Ir-Cl	2.456	2.539	P2IrN	90.62	95.55
Ir-H	1.521	1.588	P2IrCl	89.12	87.23
N-H	0.860	1.017	ClIrN	96.63	90.46
			ClIrC	175.45	169.05
			NIrC	79.24	78.58

Table S2. Vertical excitation energies, oscillator strengths and contributions (≥5%) to the electronic transitions of the two studied complexes

molecule	states	ΔE, eV (nm)	f	Assignaments
[Ir(bipy-H)]	T_1	2.84 (436)		HOMO-3 → LUMO (13%)
				HOMO → LUMO (76%)
	T_2	3.36 (368)		HOMO-4 → LUMO (3%)
				HOMO-1 → LUMO (93%)
	S_1	3.42 (362)	0.0001	HOMO-1 → LUMO (98%)
	S_2	3.43(360)	0.073	HOMO → LUMO (96%)
[Ir(bipy-H)H^+]	T_1	2.23 (534)		HOMO-2→ LUMO (23%)
				HOMO-1 → LUMO (60%)
	T_2	2.58 (479)		HOMO → LUMO+1 (98%)
	S1			
	S2			
		2.76 (449)	0.014	HOMO -2→ LUMO (2 %)
				HOMO-1 → LUMO (95%)
		2.95 (420)	0.037	HOMO -2→ LUMO (95 %)

Table S2. Ground State energy and electrochemical data for both the complexes

Complex	DFT					Experimental			
	ΔE, eV (nm)	Osc. Str.	%HOMO-LUMO	E_{HOMO}, eV	E_{LUMO}, eV	[a]E_{ox}	[a]E_{red}	[a]E_{HOMO},eV	[a]E_{LUMO},eV
[Ir(bipy-H)]	3.42 (362)	0.0001	98	-5.73	-1.62	1.37	-1.23	-5.63	-2.7
[Ir(bipy-H)H^+]	2.76 (449)	0.0140	95	-6.45	-3.12	1.34	-0.82	-5.60	-3.0

[a]All electrochemical potentials were measured in degassed 0.1 M $LiClO_4$ (supporting electrolyte) / CH_3CN solution for oxidation and reduction reactions using ferrocene / ferrocenium ion as an internal reference. HOMO (eV) = –e($E_{onsetox}$+ 4.8) V, E_g = 1240/λ, LUMO(eV) = E_g+ HOMO